Article

Discovery Medicine 2026; 38(208): 1610–1626
https://doi.org/10.24976/Discov.Med.202638208.126

RNA Binding Motif Protein 15 Regulates GTPase Activating Rap/RanGAP Domain Like 3 Gene Expression as a Potential Mechanism of Temozolomide Resistance in Glioblastoma With Epidermal Growth Factor Receptor vIII Mutation

Guoxuan Luo[1,†], Sijia Cheng[2,†], Yang Zhang[1], Jiawen Liu[1], Tingting Luo[2], Jiayi Li[2], Yunzhi Ling[2,*], Jianjun Lu[1,*]

[1]Department of Neurosurgery, The Affiliated Guangdong Second Provincial General Hospital of Jinan University, 510317 Guangzhou, Guangdong, China
[2]Research Center, Huizhou Central People's Hospital, 516001 Huizhou, Guangdong, China
*Correspondence: lyz@algaemedical.com (Yunzhi Ling); drlujianjun1978@163.com (Jianjun Lu)
[†]These authors contributed equally.
Submitted: 27 November 2025 Revised: 27 February 2026 Accepted: 18 March 2026 Published: 20 May 2026

Background: N6-methyladenosine (m6A), a type of RNA modification, influences the stability and translation of oncogene transcripts and plays a crucial role in glioblastoma (GBM) stemness and drug resistance. However, its role in epidermal growth factor receptor type III mutation (EGFRvIII) and temozolomide (TMZ)-resistant GBM remains unclear. This study explores the regulatory impact of m6A modification in TMZ-resistant GBM with EGFRvIII, with a focus on resistance genes and tumor stemness.
Methods: Stable EGFRvIII-expressing glioma cell lines were established and treated with TMZ for varying durations. Transcriptome sequencing was then performed to identify resistance-associated genes. The findings were further validated using publicly available transcriptomic datasets from TMZ-resistant GBM. Key genes related to prognosis were identified using Cox regression. The m6A modification patterns and mRNA expression-based stemness index (mRNAsi) were evaluated based on 27 m6A regulators and a one-class logistic regression model. Spearman correlation analysis assessed relationships between candidate genes, m6A scores, and mRNAsi. Cox regression analyzed prognostic differences in GBM patients with varying m6A and mRNAsi levels. U251 and A172 cells stably expressing EGFRvIII (U251OE, A172OE) were cultured, and the expression levels of *GARNL3* and *RBM15* were examined by fluorescent polymerase chain reaction and Western blotting. Furthermore, the cell proliferative capacity, viability, and apoptosis in A172OE and U251OE cells were assessed following modulation of *RBM15* expression in conjunction with TMZ treatment.
Results: *GARNL3* was identified as a drug-resistant gene in EGFRvIII-positive GBM, with high expression correlating with better overall survival ($p < 0.05$). *GARNL3* correlated with m6A scores ($p < 0.01$, $r = 0.38$) and *RBM15* ($p < 0.001$, $r = 0.992$). RBM15 promoted GARNL3 protein expression in A172OE and U251OE cells. Concurrently, knockdown of *RBM15* not only reduced *GARNL3* expression but also enhanced the proliferation and viability of A172OE and U251OE cells under TMZ treatment, while suppressing apoptosis. Conversely, overexpression of *RBM15* promoted apoptosis in these cells and enhanced the tumor-inhibitory effects of TMZ. Additionally, in TMZ-resistant EGFRvIII GBM, m6A scores were significantly decreased ($p < 0.01$), while mRNAsi scores were increased ($p < 0.001$). Low m6A and high mRNAsi levels correlated with poorer prognosis ($p < 0.05$).
Conclusion: *GARNL3* may contribute to TMZ resistance through *RBM15*-mediated m6A modification, thereby enhancing tumor cell stemness. However, this mechanism requires further validation.

Keywords: epidermal growth factor receptor vIII mutation; glioblastoma; temozolomide resistance; tumor stemness; m6A methylation modification

Introduction

Glioblastoma (GBM) is a prevalent primary intracranial tumor with high malignancy and poor prognosis, with a median survival of only 14–16 months after diagnosis [1]. Current standard treatment consists of surgical resection combined with radiotherapy and temozolomide (TMZ) chemotherapy [1]. However, GBM frequently recurs, despite treatment, and the five-year survival rate remains approximately 7% [2].

Recent gene sequencing studies on recurrent GBM following TMZ treatment have revealed that 34% to 63% of patients exhibit epidermal growth factor receptor (*EGFR*) mutations, particularly exon 2–7 deletions (EGFRvIII) [3].

The EGFRvIII mutation occurs in the later stages of GBM, leading to disease progression, poor prognosis, and TMZ resistance, as confirmed by several studies [4–7].

EGFR typically recognizes ligands such as epidermal growth factor (EGF) and transforming growth factor alpha (TGF-α) *via* its extracellular domain, activating pathways including Ras/mitogen-activated protein kinase (MAPK), phosphoinositide-3-kinase (PI3K)/Akt serine/threonine kinase (AKT), Janus kinase/signal transducer and activator of transcription (JAK/STAT), and protein kinase C (PKC) to regulate cellular activities [3,8,9]. The EGFRvIII mutation results in the loss of this extracellular domain, leading to constitutive kinase activity that can bind to wild-type *EGFR*, thereby activating traditional *EGFR* pathways and promoting GBM growth, invasion, and drug resistance [10,11]. Accordingly, EGFRvIII serves as a clinical marker of GBM progression [12]. However, current EGFRvIII-targeted treatments face challenges, including poor blood-brain barrier penetration and unexplained loss of EGFRvIII amplicon during treatment, both of which lead to suboptimal therapeutic efficacy [10]. For example, monotherapeutic approaches using early-generation small-molecule tyrosine kinase inhibitors (TKIs, e.g., erlotinib, gefitinib) or monoclonal antibodies (e.g., cetuximab) have shown minimal efficacy and low response rates in clinical trials [13]. Subsequent strategies have focused on developing more potent or specific agents as well as exploring combination therapies. For instance, the antibody-drug conjugate (ADC) Depatuxizumab Mafodotin (Depatux-M), designed to deliver a cytotoxic payload specifically to *EGFR*-overexpressing cells, was evaluated in a phase III randomized clinical trial (INTELLANCE-1) for newly diagnosed EGFR-amplified GBM. While it demonstrated a modest improvement in progression-free survival (PFS), particularly in the EGFRvIII-mutant subgroup, it ultimately failed to improve overall survival (OS) compared with the control group [14,15]. A Cochrane systematic review and meta-analysis further corroborated these findings and concluded that adding anti-EGFR therapy to the standard of care (surgery, radiotherapy, and temozolomide chemotherapy) provided no significant OS benefit in either newly diagnosed or recurrent GBM settings [16]. Therefore, understanding the molecular mechanisms of EGFRvIII-induced TMZ resistance and developing new combination therapies is crucial.

Approximately 25% of mammalian messenger RNAs undergo N6-methyladenosine (m6A), affecting RNA metabolism and regulating various cellular activities. m6A modification regulators are categorized as “writers”, “erasers”, and “readers”, which perform methylation, demethylation, and recognition of m6A modifications, respectively [17,18]. In GBM, abnormalities in m6A regulators such as *methyltransferase-like* (*METTL*) *3*, *METTL14* (writers), *AlkB homolog 5* (*ALKBH5*), *fat mass* and *obesity associated protein* (*FTO*) (erasers), and *YTH N6-methyladenosine RNA binding protein* (*YTHDF*) *2*, *YTHDF1*, *YTH domain containing 1* (*YTHDC1*), *heterogeneous nuclear ribonucleoprotein* (*HNRNP*) *C*, *HNRNPA2/B1* (readers) contribute to tumor growth, proliferation, and resistance to radiation and chemotherapy [19]. *METTL3* and *FTO* are particularly important in GBM stem cells (GSC), maintaining stemness and promoting tumor survival and resistance [20,21]. *FTO* inhibitors, such as *meclofenamic acid* (*MA2*), can suppress GSC proliferation and tumor growth in mice [22]. Moreover, *ALKBH5* overexpression, which reduces m6A levels, supports GSC maintenance and proliferation [23].

GSC is pivotal in GBM occurrence and drug resistance [24]. It is crucial to investigate whether EGFRvIII influences m6A modification and stemness maintenance in GSC. We established stable EGFRvIII-expressing glioma cell lines and induced a resistant phenotype by chronic exposure to TMZ for 14 days. Furthermore, this study examines key resistance genes using TMZ resistance-related GBM transcriptome data, exploring the correlation between EGFRvIII and m6A modification, and the role of m6A regulatory factors in regulating resistance genes.

Methods

Construction of Glioma Cell Lines Stably Expressing EGFRvIII

Retroviruses pseudotyped with an EGFRvIII-expressing vector were generated by co-transfecting 293T cells (#293T(DC), BIOSPECIES, Guangzhou, China) with the MSCV-XZ066-EGFRvIII plasmid (#20737, Addgene, Watertown, MA, USA) and the VSV-G envelope plasmid (#14888, Addgene, Watertown, MA, USA) using Lipofectamine 3000 reagent (#L3000008, Thermo Fisher Scientific, Waltham, MA, USA). The viral supernatant was collected at 72 h post-transfection. Subsequently, human glioma cell lines U251-MG (#U251-MG, BIOSPECIES, Guangzhou, China) and A172 (#A172, BIOSPECIES, Guangzhou, China) were transduced with the harvested EGFRvIII-pseudotyped retroviral particles. To select for stable integrants, the transduced cells were cultured in medium containing ampicillin (#A5354, Sigma, Burlington, MA, USA). Selection pressure was applied for approximately two weeks, with the medium refreshed every 3 days. Following this period, polyclonal populations of stably transduced cells, designated as U251OE and A172OE, were established and expanded for subsequent verification and experimental use. To confirm the successful expression of EGFRvIII in the stable transfected cell line, cell climbing slices were prepared and subjected to immunofluorescence staining. The cells were incubated with an anti-EGFRvIII primary antibody (1:500; #ab313646, Abcam, Cambridge, MA, USA), followed by a Goat Anti-Rabbit IgG H&L (Alexa Fluor® 488) secondary antibody (1:1000; #ab150081, Abcam, Cambridge, MA, USA). Nuclei were counterstained with DAPI (1 µg/mL; #D9542,

Table 1. Summary of datasets of included studies.

ID	GPL	Number of samples	Organism	Cell type
GSE140441	GPL18460	6	Homo sapiens	Two GBM patients-derived stem cells
GSE249544	GPL16791	24	Homo sapiens	Cancer stem cells and serum-differentiated cells from two GBM patients
GBM	cBioportal-TCGA	64	Homo sapiens	Tissues from GBM patients
GBM	RTCGA	170	Homo sapiens	Tissues from GBM patients

GBM, glioblastoma; GPL, Gene Expression Omnibus Platform; TCGA, The Cancer Genome Atlas.

Sigma-Aldrich, St. Louis, MO, USA). The expression and subcellular localization of EGFRvIII protein were then examined under a fluorescence microscope (Axioscope 5, Carl Zeiss, Obercohen, BW, Germany). The 293T, U251-MG, and A172 cell lines used in this study were authenticated by short tandem repeat profiling analysis and confirmed to be free of mycoplasma contamination.

Cultivation of Different Glioblastoma Cell Lines

The U251-MG, U251OE, A172, and A172OE cell lines were routinely cultured in Dulbecco's Modified Eagle Medium (containing 10% fetal bovine serum and 1% penicillin-streptomycin, #Bios-P4510, BIOSPECIES, Guangzhou, China) at 37 °C and 5% CO_2. A172OE and U251OE cells were routinely cultured until reaching the logarithmic growth phase, then treated with 100 µM or 350 µM TMZ (#AK2023-1398268, Aikang Biotechnology (Hangzhou) Co., Ltd., Hangzhou, China) for 0 (U251NC_day0, U251OE_day0), 7 (U251NC_day7, U251OE_day7), and 14 days (U251NC_day14, U251OE_day14). The culture medium was replaced every three days during the treatment period. Cells were subsequently collected for transcriptome sequencing.

Transcriptome Sequencing

With technical support from Beijing Benagen (Beijing, China), total RNA was extracted, libraries were constructed, and paired-end transcriptome sequencing (RNA-seq) was performed on all grouped cell samples ($>10^7$ cells per sample). High-quality sequencing reads were processed using fastp (v0.12.4; https://github.com/OpenGene/fastp; OpenGene, HaploX Biotechnology Co., Ltd., Shenzhen, China) and aligned to the human GRCh38 reference genome using Bowtie2 (v2.2.5, Ben Langmead Laboratory, Baltimore, MD, USA). BAM files were processed using SAMtools (v1.3.1, Harvard Medical School, Boston, MA, USA; https://github.com/samtools/samtools) for viewing, indexing, and sorting, and featureCounts (v2.0.1, Walter and Eliza Hall Institute of Medical Research, Melbourne, VIC, Australia) from the Subread package (SourceForge, San Diego, CA, USA) was employed to quantify total read counts mapped to each gene. Gene quantification results from all samples were merged, converted to transcripts per million (TPM), and $\log_2$-transformed for subsequent analysis.

Acquisition and Processing of Other Transcriptome Sequencing Datasets Related to Temozolomide-Resistant Glioblastoma

Glioblastoma transcriptome sequencing (RNA-seq) datasets were sourced from the Gene Expression Omnibus (GEO, https://www.ncbi.nlm.nih.gov/gds/), specifically including GSE140441 and GSE249544 (Table 1). Grouping was conducted according to EGFR(vIII) status and TMZ treatment. In GSE140441, GSCs were stratified into four groups: untreated EGFR-low (EGFRlowCON) and EGFR-high (EGFRhighCON) controls, along with their counterparts treated with 500 µM TMZ for 3 days (EGFRlowTMZ and EGFRhighTMZ). In GSE249544, both cancer stem-like cells (CSC) and serum-induced differentiated cells (SDC) were categorized as follows: untreated EGFR wild-type (EGFRwtCON) and EGFRvIII-positive (EGFRvIICON) controls, as well as cells treated with IC_{30} TMZ for 4 days (EGFRwtTMZ and EGFRvIIITMZ). Additionally, the GBM expression matrix (The Cancer Genome Atlas Program (TCGA)-GBM) and corresponding clinical data, comprising 64 samples treated solely with TMZ, were obtained from the cBio Cancer Genomics Portal (cBioPortal, http://www.cbioportal.org/). RNA-seq matrices of GBM and adjacent tissues were downloaded using the R editing packages "RTCGA" (v1.27.2, Marcin Kosinski, https://github.com/RTCGA/RTCGA) and "RTCGA.rnaseq.20160128" (v0.99.0, Marcin Kosinski, https://github.com/RTCGA/RTCGA.rnaseq.20160128) to screen for cancer-related genes.

The original expression matrices of the aforementioned GEO datasets represent Fragments Per Kilobase of transcript per Million mapped reads (FPKM) for over 20,000 coding genes, while the TCGA-GBM data were presented as raw counts. Subsequently, the expression matrices from these three datasets were normalized and converted to $\log_2$ TPM values. Genes with low-quality data, defined as those with a total TPM value of 0, were excluded from further analysis.

Acquisition and Functional Analysis of Temozolomide Resistance-Related Genes in Glioblastoma

For all datasets, differential expression analysis at the transcriptome level between EGFRvIII-positive GBM samples before and after TMZ treatment was conducted

using the R package "limma" (v3.48.3, Walter and Eliza Hall Institute of Medical Research, Melbourne, VIC, Australia). Genes were considered significantly differentially expressed (DEGs) if they met the criteria of adjusted *p* value or *p* value less than 0.05 and absolute differential fold change (log_2FC) greater than 1. Subsequently, the R packages "clusterProfiler" (v4.0.2, Bioconductor Project, Dana-Farber Cancer Institute, Boston, MA, USA) and "org.Hs.eg.db" (v3.13.0, Bioconductor Project, Dana-Farber Cancer Institute, Boston, MA, USA) were employed to perform enrichment analysis of DEGs in Gene Ontology (GO) terms, including Biological Process (BP), Cellular Component (CC), Molecular Function (MF), as well as Kyoto Encyclopedia of Genes and Genomes (KEGG) pathways. To identify TMZ-resistant DEGs, survival analysis was conducted using the R package "survival" (v3.2.13, Bioconductor Project, Dana-Farber Cancer Institute, Boston, MA, USA), and Cox regression was used to explore associations between DEG expression levels and clinical outcomes, such as OS and disease-free survival (DFS), in GBM patients treated with TMZ.

Variation Analysis of RNA Methylation-Related Gene Sets in Temozolomide-Resistant Glioblastoma

To assess the enrichment of m6A methylation signals in EGFRvIII-GBM samples post-TMZ treatment, gene sets related to "RNA methylation" were extracted from the Molecular Signatures Database (MSigDB, http://www.gsea-msigdb.org/gsea/index.jsp) using the R package "msigdbr" (v7.5.1, CRAN Team, Vienna, Vienna, Austria). Enrichment scores of RNA methylation, particularly m6A methylation, were calculated for each sample using the R package "GSVA" (v1.40.1, Bioconductor Project, Dana-Farber Cancer Institute, Boston, MA, USA). Differences in enrichment scores between groups were analyzed using the limma method.

M6A Methylation Score of Temozolomide-Resistant Glioblastoma

A set of 27 m6A methylation signature genes [25,26], categorized into Erasers (*ALKBH3*, *ALKBH5*, *FTO*), Writers (*zinc finger CCCH-type containing 13* (*ZC3H13*), *Vir like m6A methyltransferase associated* (*VIRMA*), *RBM15*, *RBM15B*, *METTL14*, *METTL16*, *METTL3*, *Wilms tumor 1 associated protein* (*WTAP*), *RNA binding motif protein X-linked* (*RBMX*), *Cbl proto-oncogene like 1* (*CBLL1*)), and Readers (*HNRNPA2B1*, *HNRNPC*, *HNRNPG*, *insulin like growth factor 2 mRNA binding protein* (*IGF2BP*) *1*, *IGF2BP2*, *IGF2BP3*, *YTHDC1*, *YTHDC2*, *YTHDF1*, *YTHDF2*, *YTHDF3*, *eukaryotic translation initiation factor 3 subunit A* (*EIF3A*), *fragile X mental retardation 1* (*FMR1*), *leucine rich pentatricopeptide repeat containing* (*LRPPRC*)) were identified. Principal component (PC) analysis (PCA) was performed on the expression matrix of these genes to derive PC1 and PC2 for each sample, from which an m6A score was calculated [27].

$$\text{m6A score} = \sum \text{PC1}_i + \text{PC2}_i$$

Cancer Cell Stemness Score of Glioblastoma Based on One-Class Linear Regression

To evaluate cancer cell stemness, transcriptome sequencing data from the Progenitor Cell Biology Consortium (PCBC, syn1773109) were obtained from the Synapse platform (https://www.synapse.org/Synapse:syn1773109/files/). Samples were divided into 68 human normal stem cells and 129 differentiated cells. Expression matrices were normalized to log_2 TPM values and processed using the R package "gelnet" (v1.2.1, CRAN Team, Vienna, Vienna, Austria) to build a one-class logistic regression (OCLR) model. Spearman correlation analysis using the OCLR model was applied to calculate a stemness score for each sample, which was linearly scaled to a range of 0–1 [28].

Construction of the RBM15 Overexpression Vector

The coding sequence (CDS) of human RBM15 (CCDS822.1) was chemically synthesized. The lentiviral overexpression vector pLenti-CMV-GFP-Puro (#17448, Addgene, Watertown, MA, USA) was digested with BamHI (#R3136S, NEB, Ipswich, MA, USA) and SalI (#R3138S, NEB, Ipswich, MA, USA) restriction endonucleases to generate a linearized backbone. The synthesized RBM15 CDS fragment was then ligated into the pLenti-CMV-GFP-Puro vector backbone using T4 DNA ligase (#M0202V, NEB, Ipswich, MA, USA). The resulting ligation product, pLenti-CMV-hRBM15 CDS (designated ovRBM15), was constructed with the assistance of Sangon Biotech (Shanghai) Co., Ltd. The construct was transformed into competent *E. coli* cells (#C2987I, NEB, Ipswich, MA, USA). The sequence of the RBM15 overexpression vector is provided in the **Supplementary Materials**. Positive clones were selected on LB agar plates containing ampicillin (#L0168, Sigma, Burlington, MA, USA) and subsequently verified by colony PCR and Sanger sequencing.

Detection of Differential Expression of Key Genes in Temozolomide-Resistant Glioblastoma Cells

U251OE and A172OE cells were continuously treated with 350 μM or 100 μM TMZ for 14 days, or treated with RBM15 siRNA sequence 1 (siRBM15-1: 5′-CGCAACAATGAAGGGAAAAGAGC-3′), siRNA sequence 2 (siRBM15-2: 5′-GGCCTGTTTCATGAG TTCAAACG-3′), or ovRBM15 for three days. Cells transfected with siRNA-negative sequences (siNC; sense: 5′-UUCUCCGAACGUGUCACGUTT-3′; antisense: 5′-A CGUGACACGUUCGGAGAATT-3′) and pLenti-CMV-GFP empty vector (ovNC) served as the control group. The cellular morphology was then examined under a

microscope (DM1000 LED, Leica Microsystems GmbH, Wetzlar, Hessen, Germany). Total RNA was then collected using an animal cell/tissue RNA extraction kit (#DP451-TA, Tiangen Biochemical Technology Co., Ltd., Beijing, China). The preservation of extracted RNA requires careful attention to extraction and storage temperatures, as well as the impact of repeated freeze-thaw cycles, to maintain its integrity [29,30]. Quality-controlled total RNA was first synthesized into cDNA using StarScript III one-tube genome-free reverse transcription premix reagent (#A230-02, GeneStar, Beijing, China). Then, the target primers (*GARNL3*: 5′-AACAATCAACGTGTCCCTCAAT-3′ (F), 5′-TTTGTCCAGATTCATGGCACTT-3′ (R); *RBM15*: 5′-GGCTCGCTGAGGAGAGTGGAG-3′ (F), 5′-CGGCTACTGCTCAATTCTGGACTG-3′ (R); *GAPDH*: 5′-GGAGCGAGATCCCTCCAAAAT-3′ (F), 5′-GGCTGTTGTCATACTTCTCATGG-3′ (R)), 2× RealStar Fast SYBR qPCR Mix (#A301-01, GeneStar, Beijing, China) and other qPCR reagents were mixed, and qPCR reactions were performed. The mRNA level of the target relative to *GAPDH* was calculated using the $2^{-\Delta\Delta Cq}$ formula.

Western Blotting

Following transfection with siRNAs or overexpression vectors and treatment with 100 µM or 350 µM TMZ for three days, total protein was extracted from A172OE and U251OE cells using Trizol reagent (#15596026CN, Thermo Fisher Scientific, Waltham, MA, USA). The protein concentration was quantified with a BCA protein assay kit (#KTD3001, Guangzhou LaiSai Bio, Guangzhou, China). Subsequently, 20 µg of total protein per sample was loaded onto a 10% SDS-polyacrylamide gel (#PG112, Shanghai Yamei Biomedical Technology Co., Ltd., Shanghai, China) and separated by electrophoresis at 80 V for 20 min, followed by 120 V until the proteins were adequately resolved. The proteins were then transferred onto a 0.22 µm NC membrane (#FFN56, Betoyime, Shanghai, China) at 200 mA for 100 min at 4 °C. The membrane was blocked with 5% bovine serum albumin (#A1933-25G, Sigma, Burlington, MA, USA) for 2 h, incubated with primary antibodies at 4 °C overnight, and subsequently incubated with appropriate HRP-conjugated secondary antibodies (goat anti-mouse IgG antibody, 1:1000, #A0216, Beyotime, Shanghai, China; goat anti-rabbit IgG, 1:20,000, #AB205718, Abcam, Cambridge, MA, USA) for 1 h. Protein signals were visualized using an enhanced chemiluminescence (ECL) detection reagent (#WBKLS0500, Millipore, Sigma, Burlington, MA, USA). Primary antibodies included EGFR monoclonal antibody [EP38Y] (1:1000, #ab52894, Abcam, Cambridge, MA, USA), EGFRvIII monoclonal antibody [EPR28380-83] (1:1000, #ab313646, Abcam, Cambridge, MA, USA), β-Actin (ACTB) mouse monoclonal antibody (1:2500, #AF0003, Beyotime, Shanghai, China), RBM15 monoclonal antibody (2C1) (#H00064783-M19, Thermo Fisher Scientific, Waltham, MA, USA), and GARNL3 polyclonal antibody (#PA5-55970, Thermo Fisher Scientific, Waltham, MA, USA).

Temozolomide Sensitivity Test

A172OE, U251OE cells and their respective parental cells were seeded in 96-well plates and treated with a gradient of TMZ concentrations (0, 1, 10, 50, 100, 250, 500, and 1000 µM) prepared in complete culture medium. After 72 h of continuous exposure, the medium was removed and replaced with fresh medium containing the Cell Counting Kit-8 (CCK-8) reagent (#KTA1020, Abbkine, Redlands, CA, USA). Following incubation for 1 to 4 h, the absorbance of each well was measured at a wavelength of 450 nm using a microplate reader (SpectraMax iD5, Molecular Devices, Shanghai, China). The percentage of cell viability was calculated relative to the untreated control group. A dose-response curve was plotted with the logarithm of TMZ concentration ($\log_{10}$) on the x-axis and cell viability on the y-axis, from which the half-maximal inhibitory concentration (IC_{50}) was determined.

Crystal Violet Staining

After 3 days of culture and drug treatment, cells from each treatment group (A172OE and U251OE) were fixed with 4% paraformaldehyde (#P6148, Sigma, Burlington, MA, USA) at 25 °C for 30 min. Following three washes with phosphate-buffered saline (PBS; #C0221A, Beyotime, Shanghai, China), the cells were stained with 0.5% crystal violet solution (#G5447, SmartBuffers, Foshan, China) for 10 min. The stained cells were air-dried and subsequently imaged under an optical microscope. Following solubilization of the dye with 10% acetic acid, the absorbance was measured at 570 nm on a microplate reader to calculate cell viability (%).

EdU Staining

A172OE and U251OE cells from each experimental group were incubated with culture medium containing 10 µM EdU (#ST067, Beyotime, Shanghai, China) for 2 h. The cells were then fixed with 4% paraformaldehyde for 15 min and permeabilized with 0.5% Triton X-100 (#X100, Sigma, Burlington, MA, USA) for 10 min. After another PBS wash, the click reaction cocktail containing the fluorescent azide dye, $CuSO_4$, and reaction buffer was added to the cells, which were then incubated in the dark for 30 min. Finally, the cell nuclei were counterstained with Hoechst 33342 (5 µg/mL, #C1026, Beyotime, Shanghai, China) for 10 min. The stained cells were visualized under a fluorescence microscope (Axioscope 5, Carl Zeiss, Obercohen, BW, Germany). The red fluorescence signal indicated EdU incorporation, while the blue fluorescence from Hoechst 33342 highlighted the nuclei. The average integrated op-

Table 2. Summary of clinical data of 64 glioblastoma patients treated with temozolomide.

		TMZ response (n = 23)	TMZ-resistant (n = 41)
Age (58.75, 21–84, years)		56.8 ± 16.9	56 ± 9.89
Sex	Male (n = 43)	17	26
	Female (n = 21)	6	15
IDH1	R132H (n = 6)	4	2
	WT (n = 55)	18	37
EGFR	vIII	4.348% (1/23)	12.195% (5/41)
	Others	13.043% (3/23)	19.512% (8/41)
	WT	82.609% (19/23)	68.293% (28/41)
TMB		1.26 ± 0.258	1.34 ± 0.616
MGMT	METHYLATED	12	17
	UNMETHYLATED	10	17
OS (Months)		9.71 ± 6.11	16.6 ± 11.5
DFS (Months)		9.71 ± 6.11	7.26 ± 4.80

TMZ, temozolomide; WT, wild type; OS, overall survival; DFS, disease-free/progression-free survival; EGFR, epidermal growth factor receptor; TMB, Tumor Mutational Burden; MGMT, O6-Methylguanine-DNA Methyltransferase.

tical density (IOD) value of the cell population was quantified using ImageJ software (v1.53a, National Institute of Mental Health (NIMH), Bethesda, MD, USA) to evaluate the proliferative activity.

Apoptosis Detection (Flow Cytometry)

A172OE and U251OE cells (approximately 1×10^6) were collected, washed with ice-cold PBS, and resuspended in 100 µL of binding buffer. Annexin V-FITC and PI staining solutions (#C1062M, Beyotime, Shanghai, China) were added, followed by incubation in the dark for 15 min. After adding 400 µL of binding buffer and mixing, samples were analyzed within 1 hour using a flow cytometer (BD FACSMelody™, BD, Franklin Lakes, NJ, USA). The excitation/emission wavelengths were 488/525 nm for Annexin V-FITC and 535/615 nm for PI. The apoptosis rate was quantified by calculating the percentages of Annexin V^+/PI^- (early apoptotic) and Annexin V^+/PI^- (late apoptotic) cells.

Statistical Methods

Data analysis was performed using R (v4.1.0, R Core Team 2023, Vienna, Vienna, Austria) and RStudio Server (v1.4.1717, Posit PBC, Boston, MA, USA) for visualization. Differences in gene expression levels and gene set variation analysis (GSVA) scores between groups were evaluated using empirical Bayes moderated *t*-tests, with *p* values adjusted using the *Benjamini-Hochberg* correction (*q*/*FDR* value). Functional enrichment scores were assessed using the hypergeometric distribution. Student's *t*-test was used to compare normally distributed continuous data between groups, whereas the *Mann-Whitney U* test was applied to tumor stemness scores or other continuous variables that did not meet the assumption of normality. Comparisons among multiple groups were performed using one-way analysis of variance (ANOVA) followed by *Tukey*'s multiple comparison test. A *Kruskal-Wallis H* test was conducted to assess differences across groups for non-normally distributed data, and *Dunn*'s post hoc analysis was then utilized for pairwise comparisons to identify specific group differences.

Results

Identification of Temozolomide Resistance Genes in Epidermal Growth Factor Receptor Type III Mutant Glioblastoma

We analyzed a cohort of 64 TCGA-GBM patients treated with TMZ, with ages ranging from 21 to 84 years. Males accounted for a greater proportion of the cohort than females (67.19% vs. 32.81%; 43/21). The incidence of EGFRvIII mutations, characterized by protein amplification resulting from mutations in protein sites 7–173 and exons 2–7, was higher in TMZ-resistant GBM samples (12.195%) compared with TMZ-sensitive samples (4.348%; Table 2), showing a 2.805-fold increase.

Cox regression analysis revealed that EGFRvIII mutation status was a significant risk factor for DFS in GBM patients ($p < 0.05$, **Supplementary Fig. 1B**), whereas other factors did not show significant associations (**Supplementary Fig. 1**). Specifically, EGFRvIII mutation significantly reduced DFS ($p < 0.05$, **Supplementary Fig. 1D**) but did not affect OS ($p > 0.05$, **Supplementary Fig. 1A,C**), underscoring its role in promoting TMZ resistance.

Subsequently, using the limma package, we identified 8 genes—*NIMA related kinase 6* (*NEK6*), *activated leukocyte cell adhesion molecule* (*ALCAM*), *hyaluronan synthase 2* (*HAS2*), *gamma-aminobutyric acid type A receptor subunit gamma 3* (*GABRG3*), *beaded filament structural protein 1* (*BFSP1*), *GTPase activating*

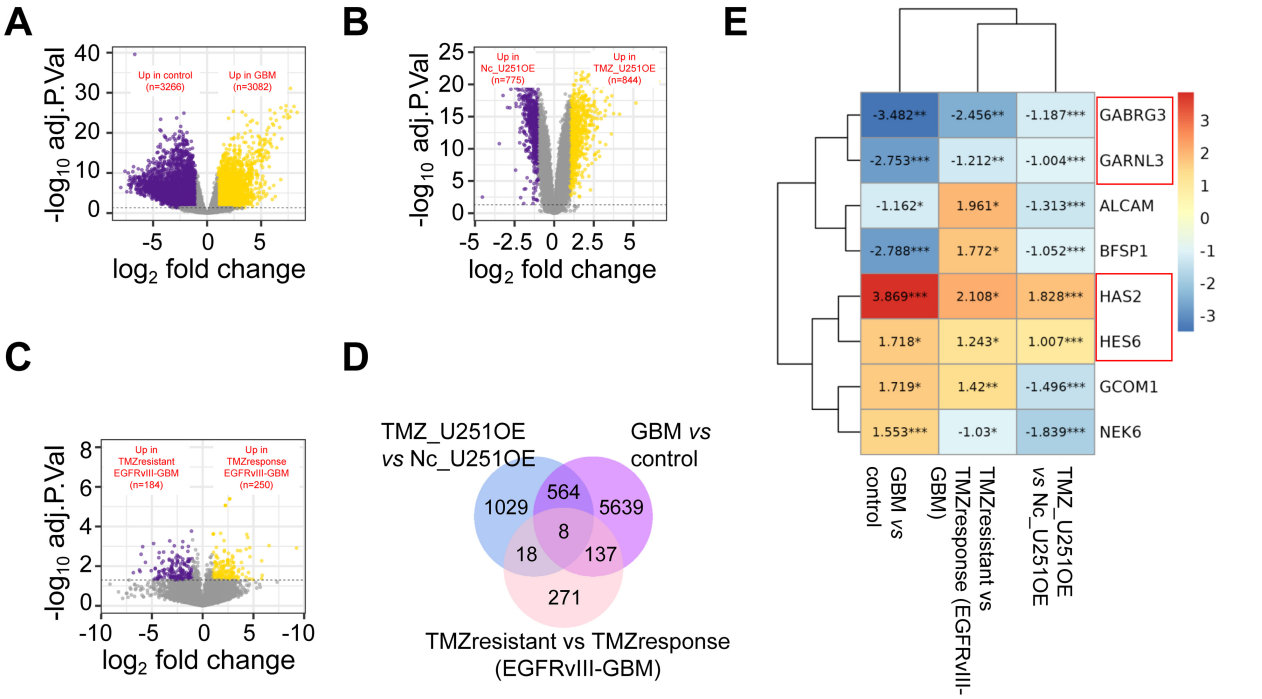

Fig. 1. Screening of temozolomide (TMZ) resistance genes in epidermal growth factor receptor type III mutant glioblastoma (GBM). (A–C) Transcriptome expression differences between GBM tumor tissues (n = 165) versus adjacent tissues (n = 5) (A), EGFRvIII-stably transduced U251 cell line (TMZ_U251OE, n = 3) treated with TMZ for 14 days versus untreated U251OE cells (Nc_U251OE, n = 3) (B), and TMZ-sensitive EGFRvIII GBM tissues versus TMZ-resistant EGFRvIII GBM tissues. (D) Venn diagram showing the overlap of differentially expressed genes in (A–C). (E) Log_2 fold change (log_2FC) in expression of 8 TMZ resistance genes across GBM models, highlighting consistent trends in *GABRG3*, *GARNL3*, *HAS2*, and *HES6*. * $p < 0.05$; ** $p < 0.01$; *** $p < 0.001$.

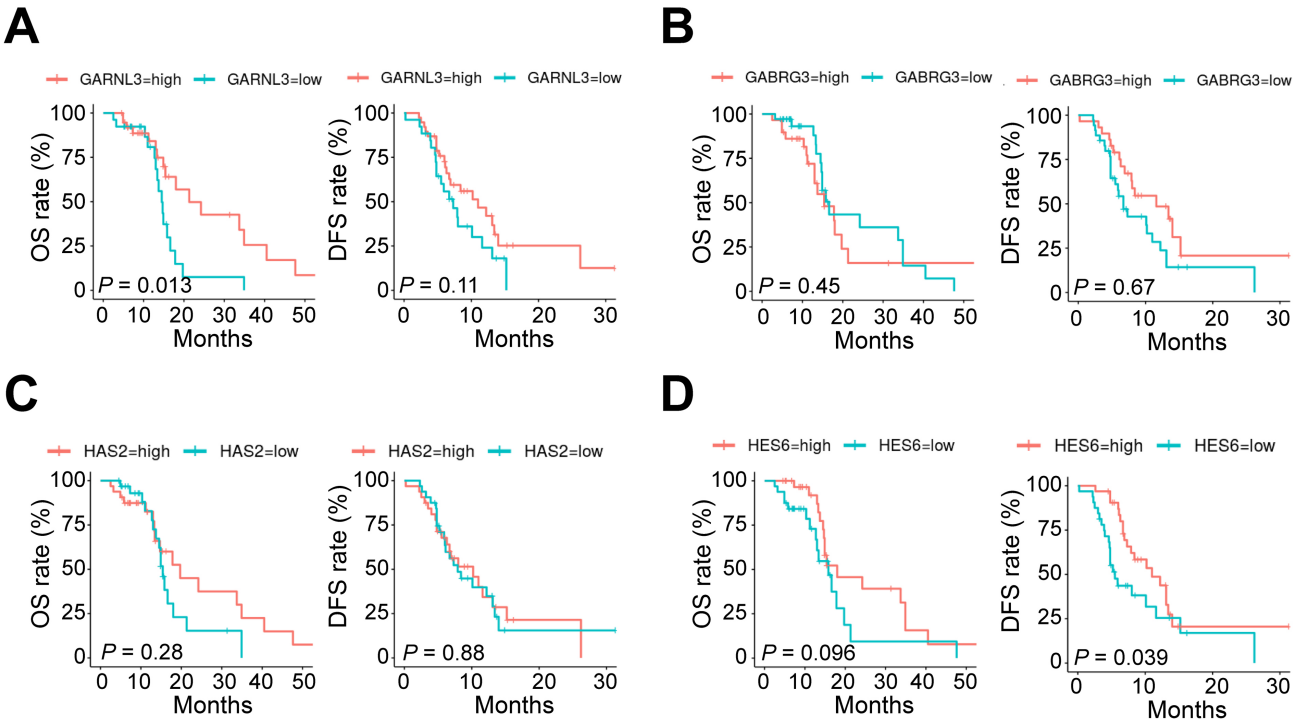

Fig. 2. Correlation between expression levels of four key temozolomide resistance genes and glioblastoma (GBM) patient prognosis. (A–D) Overall survival (OS) and disease-free survival (DFS) differences in GBM patients stratified by expression levels of *GARNL3* (A), *GABRG3* (B), *HAS2* (C), and *HES6* (D).

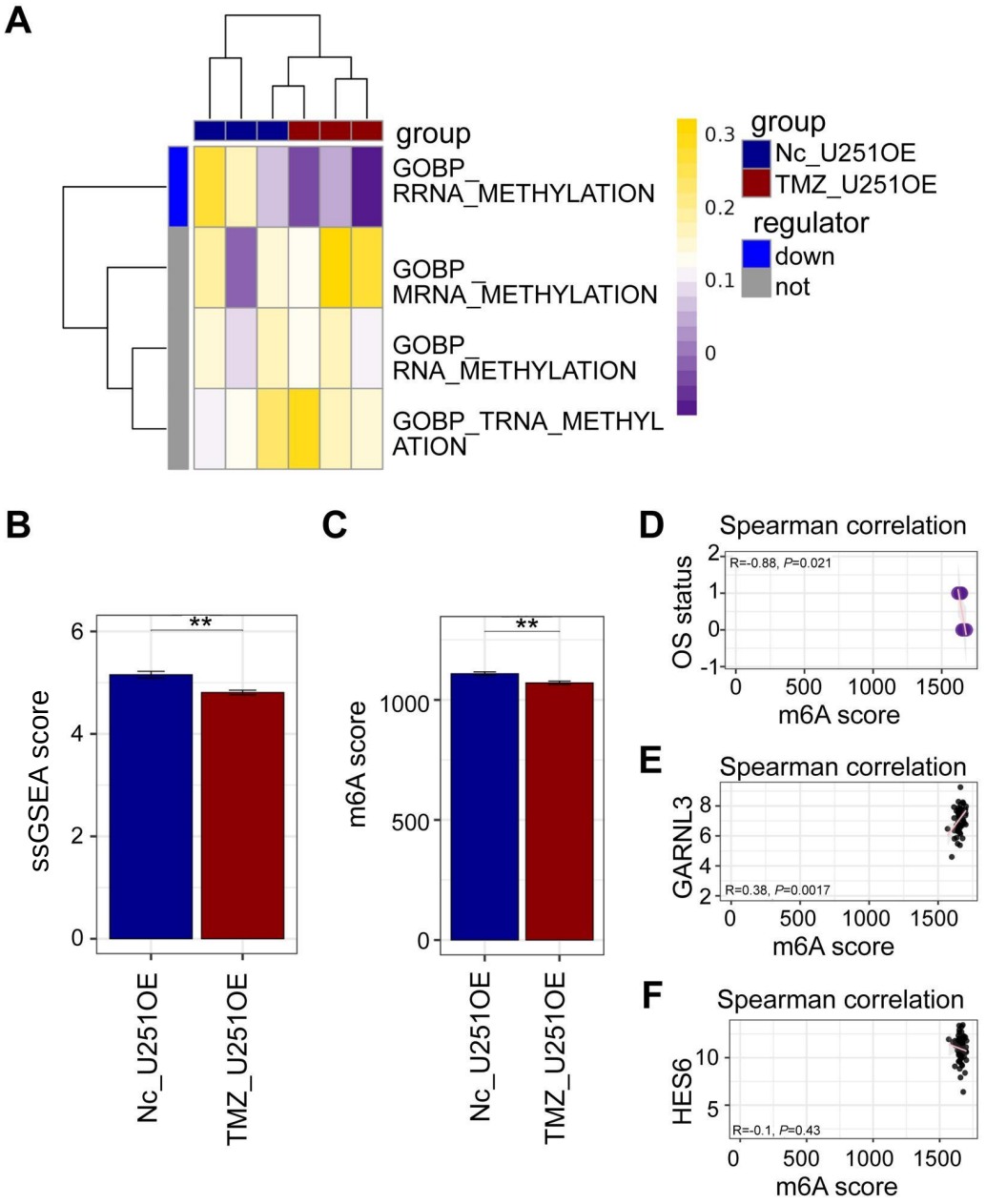

Fig. 3. Diminished m6A signature gene enrichment in temozolomide (TMZ)-resistant glioblastoma (GBM) with epidermal growth factor receptor exon 2–7 deletion (EGFRvIII). (A) The gene set variation analysis scores of RNA methylation-related biological processes (BP) that are enriched in the transcriptome expression profiles of EGFRvIII-stably transduced U251 cell line (U251OE) before and after TMZ treatment. (B,C) Single-sample gene set enrichment analysis (ssGSEA) score (B) and m6A score (C) of m6A methylation signal in genes of U251OE cells before and after TMZ treatment. (D–F) Correlation of m6A fraction with overall survival (OS, D), *GARNL3* (E), and *HES6* (F) expression levels in EGFRvIII-GBM patients (n = 64). ** $p < 0.01$.

Rap/RanGAP domain like 3 (*GARNL3*), *Hes family bHLH transcription factor 6* (*HES6*), and *glutamate receptor ionotropic NMDA like subunit 1-associated protein 1 complex locus 1* (*GCOM1*)—that were significantly differentially expressed between GBM tumors and TMZ-resistant EGFRvIII-positive GBM tissues. These findings were validated using the U251OE cell model (Fig. 1A–D). Notably, GABRG3 and GARNL3 were consistently downregulated ($p < 0.01$ or 0.001, $\log_2$FC <-1) in TMZ-resistant EGFRvIII-GBM tissues and U251OE cell lines, while HAS2 and HES6 were consistently upregulated ($p < 0.05$ or 0.001, $\log_2$FC >1, Fig. 1E). These genes—GABRG3, GARNL3, HAS2, and HES6—were identified as candidate genes for TMZ resistance in EGFRvIII-positive GBM.

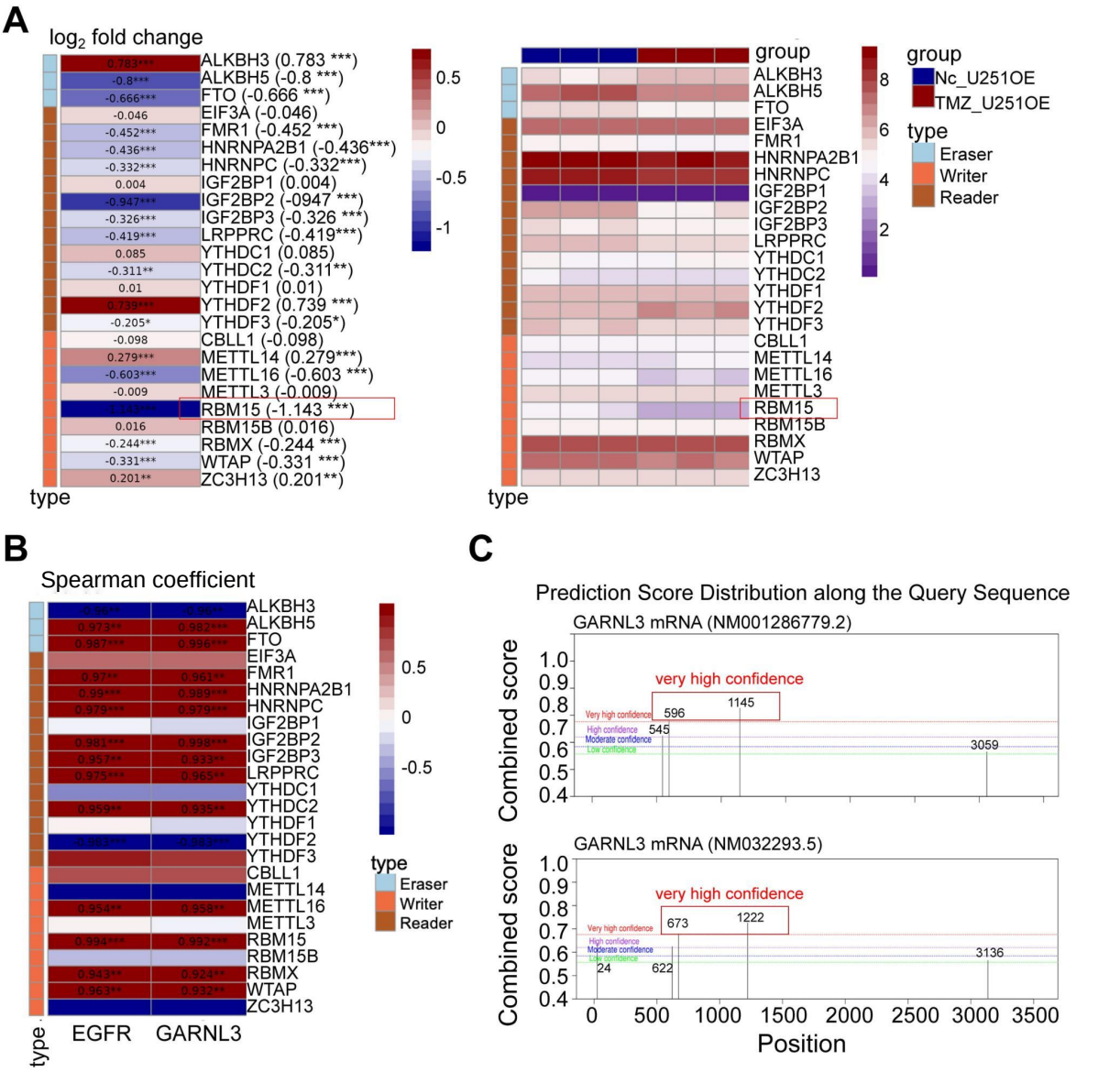

Fig. 4. Expression of m6A methylation signature genes in epidermal growth factor receptor vIII (EGFRvIII) mutant glioblastoma. (A) Log_2 fold change (left) and log_2 transcripts per million values (right) for 27 characteristic genes in EGFRvIII-stably transduced U251 cell line (U251OE) before and after temozolomide (TMZ) treatment, with a focus on *RBM15*. (B) Spearman correlation analysis between the 27 characteristic genes of m6A methylation and the expression levels of *GARNL3* and *EGFR*. (C) prediction of m6A modification sites in *GARNL3* using sequence-based RNA adenosine methylation site predictor database (SRAMP, http://www.cuilab.cn/sramp). *, **, and *** represent $p < 0.05$, $p < 0.01$, or $p < 0.001$, respectively.

Further prognostic analysis of these candidate genes revealed that *GARNL3* was significantly associated with OS in GBM patients following TMZ treatment ($p < 0.05$, Fig. 2A). However, expression levels of the other two candidate genes (*GABRG3* and *HAS2*) did not show significant associations with OS or DFS ($p > 0.05$, Fig. 2B,C). Although higher expression of *HES6* was significantly associated with improved DFS ($p < 0.05$, Fig. 2D), the strength of this association was notably lower compared with that of *GARNL3*. These findings highlight *GARNL3* as a key gene contributing to TMZ resistance in EGFRvIII-positive GBM, and suggest that its upregulation may potentially improve OS in patients.

Correlation Between m6A Methylation and Temozolomide Resistance Gene Expression in Epidermal Growth Factor Receptor Type III Mutant Glioblastoma

The m6A modification plays a pivotal role in RNA metabolism, affecting functional genes associated with can-

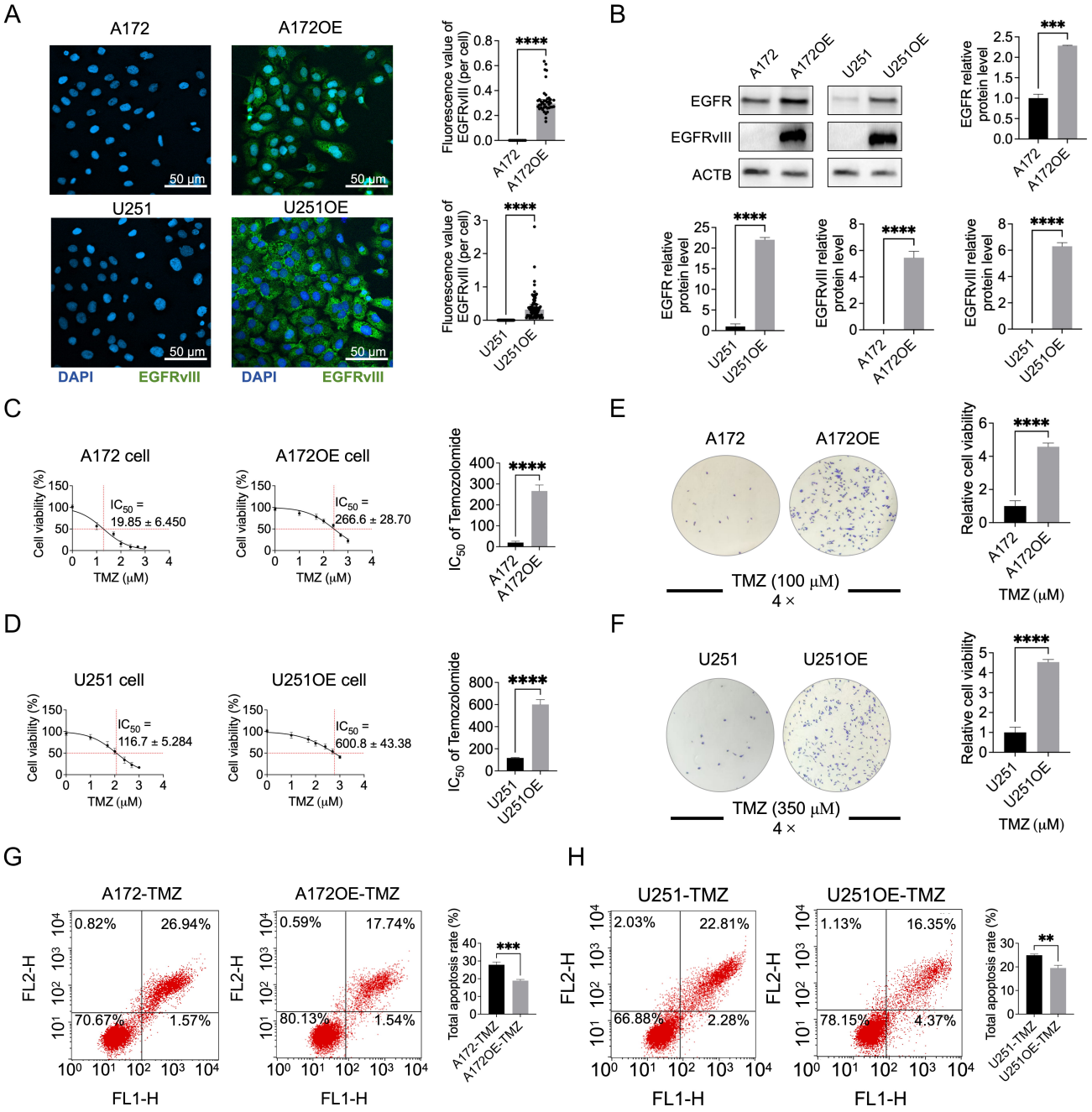

Fig. 5. The effect of epidermal growth factor receptor type III (EGFRvIII) mutation on the sensitivity of glioblastoma cells to temozolomide (TMZ). (A,B) Representative micrographs (20×, A) and immunoblotting (B) for detecting EGFRvIII in stably transfected A172 and U251 human glioma cells. (C,D) Half-maximal inhibitory concentration (IC_{50}) curves of TMZ in EGFRvIII-overexpressing A172 cells (A172OE, C), U251 cells (U251OE, D), and their respective parental cells. (E,F) Representative crystal violet staining images (4×) of A172OE and A172 cells treated with 100 μM TMZ (E), U251OE and U251 cells treated with 350 μM TMZ (F) for 3 days. (G,H) Analysis of apoptosis by flow cytometry in A172OE and A172 cells (G), U251OE and U251 cells (H) following TMZ treatment. **, *** and **** represent $p < 0.01$, 0.001 and 0.0001, respectively.

cer stem cell renewal, tumor invasion, and treatment evasion [31]. Our analysis revealed a significant reduction in rRNA methylation and the fraction of m6A methylation signals enriched in the U251OE cell line treated with TMZ for 14 days (Fig. 3A–C). Concurrently, a strong negative correlation was observed between the m6A fraction and the survival of EGFRvIII-positive GBM patients ($p < 0.05$, $r < –0.8$, Fig. 3D), suggesting that decreased m6A signaling may indicate poorer prognosis.

Moreover, in GBM patients treated with TMZ, *GARNL3* exhibited a weak but statistically significant positive correlation with the m6A score ($p < 0.01$, $r < 0.3$,

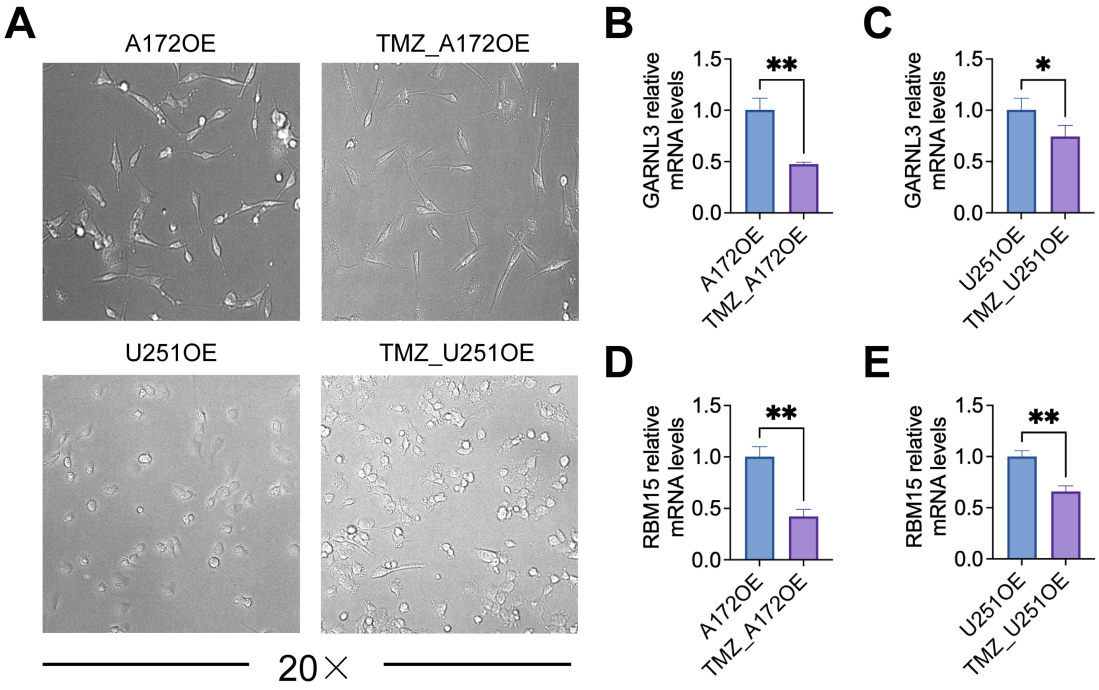

Fig. 6. Expression changes of target genes in glioblastomas with epidermal growth factor receptor type III (EGFRvIII) mutation or temozolomide (TMZ) resistance. (A) The morphology of A172 and U251 cells in each group under the microscope (20×). (B,C) Expression changes and differences of *GARNL3* mRNA in EGFRvIII-type A172 (A172OE, n = 3 per group; B) and U251 cells (U251OE, n = 3 per group; C) cells after 14 days of TMZ treatment. (D,E) Expression changes and differences of *RBM15* mRNA in A172OE cells (n = 3 per group; D) and U251OE cells (n = 3 per group; E) after 14 days of TMZ treatment. * and ** represent $p < 0.05$ and $p < 0.01$, respectively.

Fig. 3E). In contrast, there was no significant correlation between *HES6* and the m6A fraction ($p > 0.05$, Fig. 3F). These findings were confirmed in the TMZ_U251OE cell line, where *GARNL3* downregulation coincided with a notable decrease in the m6A levels. This indicates potential involvement of m6A modification in regulating *GARNL3* mRNA metabolism in TMZ-resistant EGFRvIII-GBM.

Notably, *RBM15*, as an m6A modification signature gene, exhibited significantly low expression in the TMZ_U251OE cell line ($p < 0.001$, Fig. 4A) and demonstrated a strong positive correlation with *GARNL3* ($p < 0.001$, $r > 0.99$, Fig. 4B). While the other 25 m6A modification characteristic genes showed minimal differential expression in the U251OE cell line ($|\log_2 FC| < 1$), *RBM15* emerged as potentially crucial for maintaining the stability of *GARNL3* mRNA. Furthermore, predictive analysis using the SRAMP tool indicated that m6A-binding proteins may regulate *GARNL3* by targeting specific sites on its mRNA. High-confidence putative m6A modification sites were identified at positions 673 and 1222 in the *GARNL3*-NM032293.5 transcript variant, and at positions 596 and 1145 of the *GARNL3*-NM001286779.2 transcript variant (Fig. 4C).

Preliminary Verification of Significant Downregulation of GARNL3 and RBM15 in Temozolomide-Resistant Glioblastoma

The sensitivity of the stably transfected A172OE and U251OE cell lines (Fig. 5A–D) to TMZ was evaluated. Compared with their parental cells (A172 and U251), A172OE and U251OE cells' sensitivity was significantly decreased ($p < 0.0001$, Fig. 5C,D). Consistent with this, microscopic observation revealed a higher viability rate in A172OE and U251OE cells compared with their parental counterparts under TMZ treatment ($p < 0.0001$, Fig. 5E,F). Furthermore, total apoptosis rates were markedly reduced in A172OE ($p < 0.001$, Fig. 5G) and U251OE cells ($p < 0.01$, Fig. 5H). These results indicate reduced sensitivity of A172OE and U251OE cells to TMZ.

Both A172OE and TMZ-treated A172OE cells displayed a spindle-shaped morphology and adhered to the culture surface, with no obvious morphological differences between them. U251OE and TMZ-treated U251OE cells were predominantly round or oval in shape. Compared with A172OE/U251OE cells, TMZ-induced cells exhibited higher density and grew in clusters under the same culture conditions and duration (Fig. 6A). We further examined the expression levels of *GARNL3* and *RBM15* in these different cell lines. The results showed that, compared with the con-

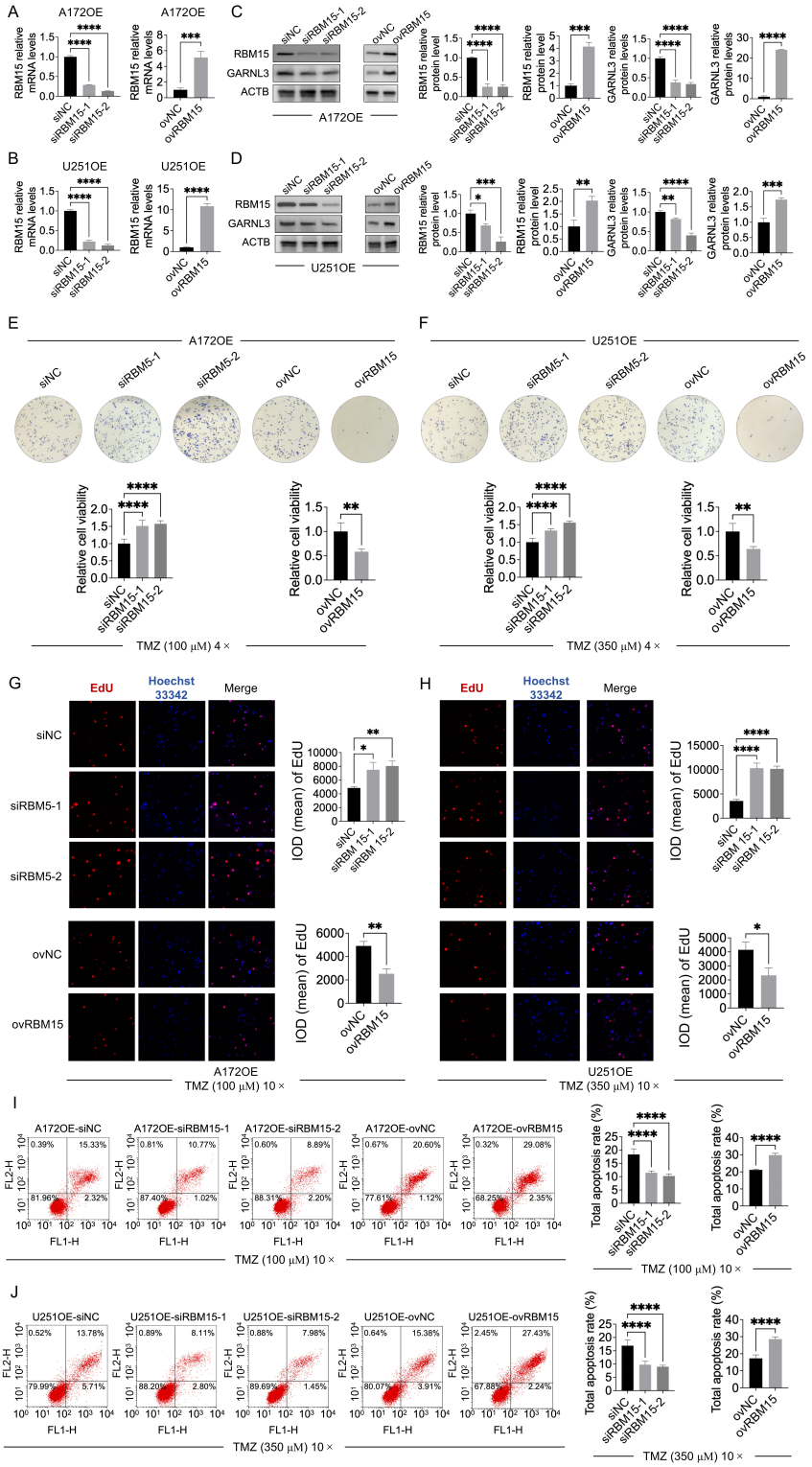

Fig. 7. The effect of interfering with RBM15 expression on the sensitivity of epidermal growth factor receptor type III (EGFRvIII) mutated glioblastoma to temozolomide (TMZ). (A,B) Relative mRNA expression levels of RBM15 in A172OE and U251OE cells after treatment with siRNA or overexpression vectors for 3 days. (C,D) Protein expression levels of RBM15 and GARNL3 in A172OE and U251OE cells following RBM15 knockdown or overexpression. (E,F) Representative crystal violet staining images (4×) of A172OE and U251OE cells treated with RBM15 siRNAs or overexpression vector, each in combination with TMZ. (G,H) Mean integrated optical density (IOD) values of EdU staining in A172OE and U251OE cells after modulation of RBM15 expression combined with TMZ treatment. (I,J) Apoptosis analysis by flow cytometry in A172OE and U251OE cells following RBM15 intervention combined with TMZ treatment. *, **, *** and **** represent $p < 0.05$, $p < 0.01$, $p < 0.001$ and $p < 0.0001$, respectively.

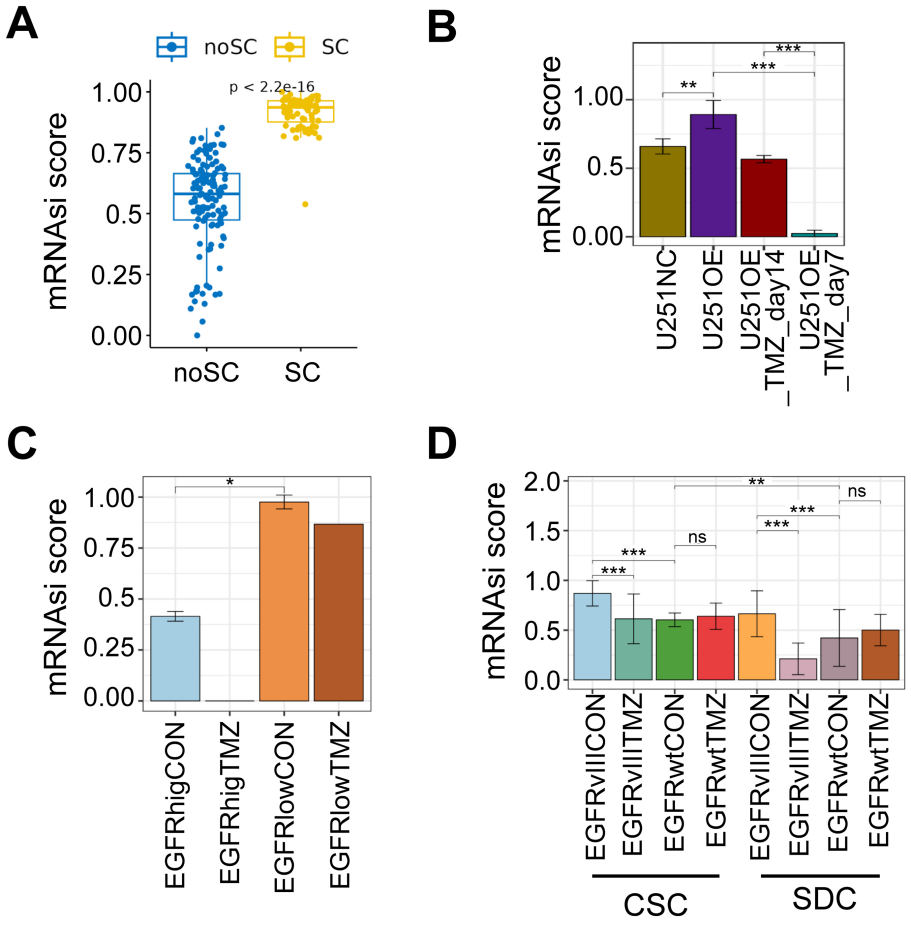

Fig. 8. Effect of epidermal growth factor receptor vIII mutation on stemness of glioblastoma (EGFRvIII-GBM). (A) Score differences of the tumor stemness score (mRNAsi) model based on the progenitor cell biology consortium (PCBC) dataset. (B–D) Changes in tumor stemness in U251 cell line stably expressing EGFRvIII after TMZ treatment (U251OE, B), patient-derived GBM stem cells (GSE140441, C), and serum-differentiated cells (GSE249544, D). ns represents $p > 0.05$; *, ** and *** represent $p < 0.05$, $p < 0.01$ and $p < 0.001$, respectively. mRNAsi, mRNA expression-based stemness index.

trol group (A172OE and U251OE), *GARNL3* mRNA was significantly downregulated in TMZ-resistant EGFRvIII glioma cells A172 (TMZ_A172OE, $p < 0.01$, Fig. 6B) and U251 cells (TMZ_U251OE, $p < 0.05$, Fig. 6C), and *RBM15* was also significantly downregulated ($p < 0.01$, Fig. 6D,E). These findings suggest that *RBM15* and *GARNL3* show consistent expression changes in TMZ-resistant EGFRvIII GBM cells.

Furthermore, knockdown of RBM15 in A172OE ($p < 0.0001$) and U251OE ($p < 0.0001$) cells (Fig. 7A–D) was accompanied by a relative decrease in GARNL3 protein levels (Fig. 7C,D). Crystal violet staining revealed that, under TMZ treatment, reduced RBM15 expression led to higher cell viability rate in A172OE (Fig. 7E) and U251OE (Fig. 7F) cells compared with the siNC group. Consistent with this, EdU staining also showed significantly increased proliferative capacity in siRNA-treated A172OE ($p < 0.05$ or 0.01, Fig. 7G) and U251OE ($p < 0.0001$, Fig. 7H) cells. In contrast, total apoptosis rates were markedly reduced (Fig. 7I,J). Conversely, overexpression of RBM15 increased GARNL3 protein levels (Fig. 7C,D), and significantly inhibited the cell viability in A172OE ($p < 0.01$, Fig. 7E,G) and U251OE ($p < 0.05$, Fig. 7F,H) cells. Moreover, the total apoptosis rate was significantly increased ($p < 0.0001$, Fig. 7I,J) in A172OE and U251OE cells after RBM15 overexpression. These results preliminarily indicated that in EGFRvIII-positive GBM cells, RBM15 positively regulates the protein level of GARNL3 and could enhance the inhibitory effect of TMZ.

The Regulatory Effect of m6A Modification on Cancer Stem Cell Differentiation in Epidermal Growth Factor Receptor Type III Mutant Glioblastoma

Consistent with the findings above, the m6A signal enrichment fraction was significantly attenuated in GBM stem cells harboring EGFRvIII mutation following TMZ treatment ($p < 0.05$, **Supplementary Fig. 2** and **Supplementary Fig. 3B**). A similar downward trend was observed in GBM stem cells with EGFR amplification and expression;

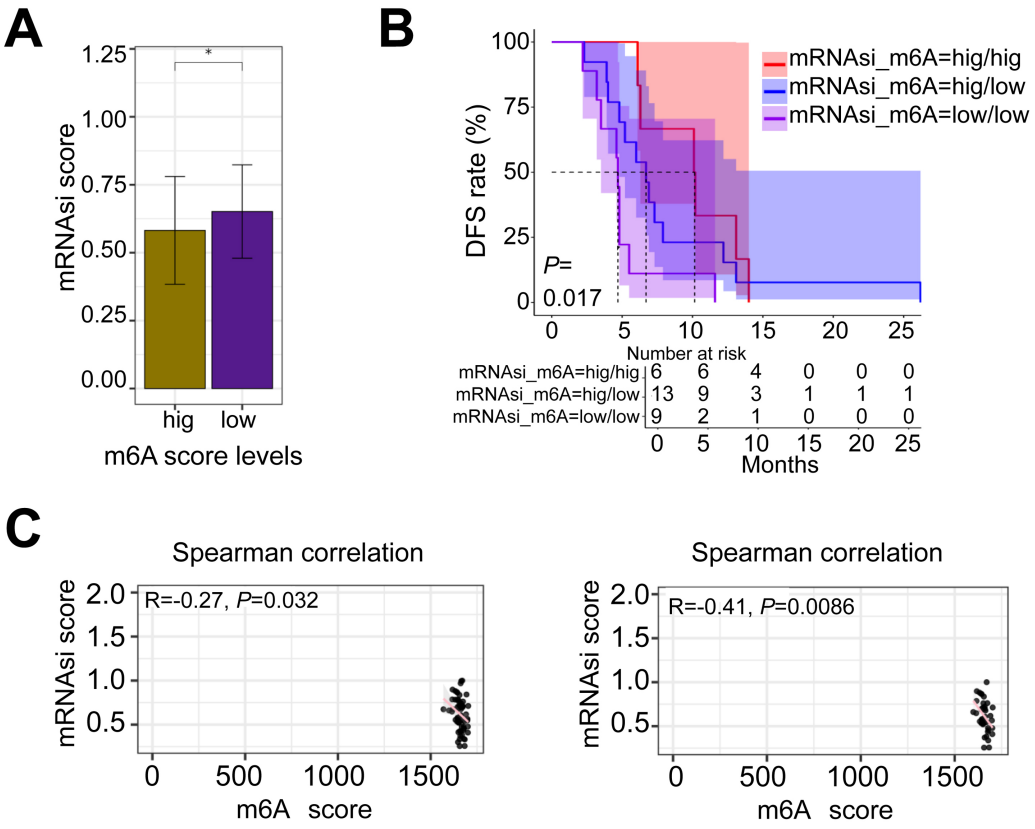

Fig. 9. Tumor cell stemness (mRNAsi) associated with m6A modification and prognosis in glioblastoma (GBM) patients. (A) Differences in mRNAsi scores in GBM patient tissues with varying m6A fraction levels (n = 64) treated with temozolomide (TMZ). (B) Median disease-free survival (DFS) period differences in patients with different m6A levels. (C) Spearman correlation analysis between mRNAsi and m6A scores in TMZ-treated (left panel) and TMZ-resistant (right panel) GBM patients. * indicates $p < 0.05$. mRNA expression-based stemness index (mRNAsi).

however, the difference was not statistically significant ($p > 0.05$, **Supplementary Fig. 3A**), possibly due to sample heterogeneity and the limited number of included samples.

Furthermore, an OCLR model was constructed to assess tumor stemness scoring, demonstrating high evaluation accuracy ($p < 0.001$, Fig. 8A). Further analysis of the correlation between EGFRvIII and tumor stemness, along with comparisons of EGFRvIII and wild-type mRNA expression-based stemness index (mRNAsi), revealed that expression of EGFRvIII significantly improved the mRNAsi score of U251 cells compared with their wild-type counterparts ($p < 0.01$; Fig. 8B). A significant increase in mRNAsi scores was also observed in GBM stem cells derived from patients with low EGFR expression and low TMZ sensitivity, compared with those from patients with high EGFR expression ($p < 0.05$, Fig. 8C), as well as in EGFRvIII-positive CSC and EGFRvIII-positive SDC ($p < 0.001$, Fig. 8D). The EGFRvIII mutation may thus augment the stemness of GBM cells. Additionally, short-term treatment of TMZ-exposed CSC (CSC-EGFRvIIITMZ) and SDC (SDC-EGFRvIIITMZ) from GBM patients for four days ($p < 0.001$, Fig. 8D), and U251OE cells for 7 days ($p < 0.001$, Fig. 8B), initially reduced mRNAsi scores. However, prolonged treatment of U251OE cells significantly improved mRNAsi score ($p < 0.001$, Fig. 8B), suggesting a propensity of cancer cells to regain stemness over time.

Regarding m6A modification and mRNAsi, GBM tissues exhibited elevated mRNAsi levels in samples and low m6A scores ($p < 0.05$, Fig. 9A), with a significant negative correlation observed between m6A and mRNAsi ($p < 0.05$, $r = –0.27$; $p < 0.01$, $r = –0.41$, Fig. 9B,C). Moreover, among TMZ-resistant patients, those with mRNAsi high/m6A low and mRNAsi low/m6A low profiles showed poorer prognosis ($p < 0.05$, Fig. 9B). These findings collectively suggest that aberrant attenuation of m6A may enhance GBM cell stemness, adversely affecting patient survival.

Discussion

Our analysis of clinical data from 64 GBM patients treated with TMZ revealed a high *EGFR* mutation rate of 26.563% (17/64), with EGFRvIII mutations accounting for 35.294% (6/17). Particularly among TMZ-resistant GBM patients, the proportion of EGFRvIII-positive cases increased from 4.348% to 12.195%. Consistent with previous studies, EGFRvIII mutation contributes to TMZ resis-

tance in GBM [32], leading to poorer prognosis [7]. Various EGFRvIII-targeted antitumor therapies, such as EGFRvIII - CART, CDX-110-KLH peptide vaccine, and monoclonal antibodies, have shown promising anticancer effects at the cellular level [33,34], with successful outcomes in clinical and preclinical studies. However, the clinical guidelines for GBM diagnosis and treatment do not recommend EGFRvIII inhibitors, partly due to challenges in drug delivery across the blood-brain barrier and the heterogeneity among patients [35,36]. Thus, further elucidating the mechanisms of EGFRvIII resistance in GBM remains pivotal in oncology research.

Our study identifies *GARNL3* as a key resistance gene in EGFRvIII GBM. Consistent findings from other data mining studies also underscore *GARNL3* as a pivotal gene in GBM [37]. Building on our previous research, we confirmed that *GARNL3* is significantly underexpressed in EGFRvIII-stable U87 cell lines, which correlates with reduced sensitivity to TMZ across multiple cell models, including U87 and U251 [38]. While the precise role of *GARNL3* in tumorigenesis remains unclear, structural predictions suggest potential GTPase-activating protein (GAP) activity. GAPs negatively regulate GTPases by converting active GTPase-GTP forms to inactive GTPase-GDP forms [39], thereby inhibiting downstream signaling pathways and regulating cell proliferation. Dysregulation of GAP proteins has been implicated in various malignancies, including GBM, promoting tumor invasion [40]. Thus, loss of *GARNL3* may mediate GBM progression and drug resistance.

Our analysis further implicates the downregulation of *GARNL3* in TMZ-resistant GBM with weakened m6A signaling, particularly due to reduced expression of *RBM15*. *RBM15*, known for its regulatory role in mRNA post-transcriptional fate, is involved in carcinogenesis, stemness maintenance, and therapeutic response in GBM [41,42]. *RBM15* has been identified as an oncogene in various cancers, stabilizing oncogenic transcripts such as *TMBIM6*, *MyD88*, and *MDR1* [43–45], and inhibiting differentiation in leukemic stem cells and macrophages [46]. In our study, we observed significant downregulation of *RBM15* in drug-resistant samples, likely contributing to enhanced GBM stemness and TMZ resistance. Studies have also shown that reduced *RBM15* levels in GBM diminish m6A modification of *DLG3* mRNA, promoting GBM progression and radioresistance [47]. This underscores the role of *RBM15* in regulating cell stemness through m6A modification.

Moreover, our findings highlight the significance of m6A modification in GBM adaptation to cellular stressors, including therapy. Studies indicate increased m6A modification in TMZ-resistant GBM cells, attributed to *METTL3* upregulation following TMZ treatment [48]. Conversely, enhanced GSC stemness in TMZ resistance correlates with diminished m6A modification. The diverse roles of m6A regulatory factors likely contribute to these differences.

This research underscores the intricate interplay between EGFRvIII mutations, *GARNL3*, *RBM15*, and m6A modification in GBM pathogenesis and therapeutic resistance. Further investigation of these molecular mechanisms is crucial for developing targeted therapies to overcome EGFRvIII-mediated resistance and improve outcomes in GBM patients.

Conclusion

In conclusion, our study identified *GARNL3* as a critical prognostic biomarker in EGFRvIII GBM resistance, with its downregulation in drug-resistant samples potentially linked to aberrant m6A modification due to *RBM15* loss. This study is the first to connect *GARNL3*-mediated TMZ resistance in EGFRvIII GBM with the maintenance of GSC stemness. *RBM15* downregulation likely reduces *GARNL3* m6A modification, destabilizing mRNA and regulating the maintenance and stability of cancer stem cells.

Availability of Data and Materials

Data were retrieved from the publicly accessible GEO database (https://www.ncbi.nlm.nih.gov/gds/), including the GSE140441 and GSE249544 datasets, both of which are available for download from the site.

Author Contributions

GXL and SJC conceived and designed the study, developed the methodology, performed the experiments, and drafted the original manuscript. YZ, JWL, TTL, and JYL primarily handled data collection and analysis. YZL contributed to the study design and offered critical revisions and manuscript refinement. JJL was involved in establishing the study concept, designed this study, and provided funding support. All authors contributed to important editing of the manuscript and approved the final version for publication. All authors have participated sufficiently in the work to take public responsibility for appropriate portions of the content and agreed to be accountable for all aspects of the work in ensuring that questions related to its accuracy or integrity.

Ethics Approval and Consent to Participate

Not applicable.

Acknowledgment

The authors thank all the staff who have contributed to this research.

Funding

This study was supported by Basic and Applied Basic Research Project (202201020514), (Dengfeng

Hospital) Basic Research Project (SL2023A03J00689) of Guangzhou City School (Institute) Joint Funding Project, Science and Technology Planning Project of Guangzhou (2023A03J0264), Guangdong Medical Research Foundation (B2023037), Guangdong Basic and Applied Basic Research Foundation (2023B1515120085, 2024A1515110272 and 2022A1515110197), and Shenzhen Science and Technology Innovation Commission (JCYJ20220530152008019).

Conflict of Interest

The authors declare no conflict of interest.

Supplementary Material

Supplementary material associated with this article can be found, in the online version, at https://doi.org/10.24976/Discov.Med.202638208.126.

References

[1] McKinnon C, Nandhabalan M, Murray SA, Plaha P. Glioblastoma: clinical presentation, diagnosis, and management. BMJ (Clinical Research Ed.). 2021; 374: n1560. https://doi.org/10.1136/bmj.n1560.

[2] Schaff LR, Mellinghoff IK. Glioblastoma and Other Primary Brain Malignancies in Adults: A Review. JAMA. 2023; 329: 574–587. https://doi.org/10.1001/jama.2023.0023.

[3] Gan HK, Cvrljevic AN, Johns TG. The epidermal growth factor receptor variant III (EGFRvIII): where wild things are altered. The FEBS Journal. 2013; 280: 5350–5370. https://doi.org/10.1111/febs.12393.

[4] Keller S, Schmidt MHH. EGFR and EGFRvIII Promote Angiogenesis and Cell Invasion in Glioblastoma: Combination Therapies for an Effective Treatment. International Journal of Molecular Sciences. 2017; 18: 1295. https://doi.org/10.3390/ijms18061295.

[5] Zadeh G, Bhat KPL, Aldape K. EGFR and EGFRvIII in glioblastoma: partners in crime. Cancer Cell. 2013; 24: 403–404. https://doi.org/10.1016/j.ccr.2013.09.017.

[6] Pan PC, Magge RS. Mechanisms of EGFR Resistance in Glioblastoma. International Journal of Molecular Sciences. 2020; 21: 8471. https://doi.org/10.3390/ijms21228471.

[7] Shi ZF, Li GZ, Zhai Y, Pan CQ, Wang D, Yu MC, *et al*. EGFRvIII Promotes the Proneural-Mesenchymal Transition of Glioblastoma Multiforme and Reduces Its Sensitivity to Temozolomide by Regulating the NF-κB/ALDH1A3 Axis. Genes. 20234; 14: 651. https://doi.org/10.3390/genes14030651.

[8] Wee P, Wang Z. Epidermal Growth Factor Receptor Cell Proliferation Signaling Pathways. Cancers. 2017; 9: 52. https://doi.org/10.3390/cancers9050052.

[9] Villa GR, Mischel PS. Old player, new partner: EGFRvIII and cytokine receptor signaling in glioblastoma. Nature Neuroscience. 2016; 19: 765–767. https://doi.org/10.1038/nn.4302.

[10] An Z, Aksoy O, Zheng T, Fan QW, Weiss WA. Epidermal growth factor receptor and EGFRvIII in glioblastoma: signaling pathways and targeted therapies. Oncogene. 2018; 37: 1561–1575. https://doi.org/10.1038/s41388-017-0045-7.

[11] Huang K, Liu X, Li Y, Wang Q, Zhou J, Wang Y, *et al*. Genome-Wide CRISPR-Cas9 Screening Identifies NF-κB/E2F6 Responsible for EGFRvIII-Associated Temozolomide Resistance in Glioblastoma. Advanced Science. 2019; 6: 1900782. https://doi.org/10.1002/advs.201900782.

[12] Camara-Quintana JQ, Nitta RT, Li G. Pathology: commonly monitored glioblastoma markers: EFGR, EGFRvIII, PTEN, and MGMT. Neurosurgery Clinics of North America. 2012; 23: 237–246, viii. https://doi.org/10.1016/j.nec.2012.01.011.

[13] Cooper AJ, Sequist LV, Lin JJ. Third-generation EGFR and ALK inhibitors: mechanisms of resistance and management. Nature Reviews. Clinical Oncology. 2022; 19: 499–514. https://doi.org/10.1038/s41571-022-00639-9.

[14] Narita Y, Muragaki Y, Kagawa N, Asai K, Nagane M, Matsuda M, *et al*. Safety and efficacy of depatuxizumab mafodotin in Japanese patients with malignant glioma: A nonrandomized, phase 1/2 trial. Cancer Science. 2021; 112: 5020–5033. https://doi.org/10.1111/cas.15153.

[15] Lassman AB, Pugh SL, Wang TJC, Aldape K, Gan HK, Preusser M, *et al*. Depatuxizumab mafodotin in EGFR-amplified newly diagnosed glioblastoma: A phase III randomized clinical trial. Neuro-oncology. 2023; 25: 339–350. https://doi.org/10.1093/neuonc/noac173.

[16] Lee A, Arasaratnam M, Chan DLH, Khasraw M, Howell VM, Wheeler H. Anti-epidermal growth factor receptor therapy for glioblastoma in adults. The Cochrane Database of Systematic Reviews. 2020; 5: CD013238. https://doi.org/10.1002/14651858.CD013238.pub2.

[17] Boulias K, Greer EL. Biological roles of adenine methylation in RNA. Nature Reviews. Genetics. 2023; 24: 143–160. https://doi.org/10.1038/s41576-022-00534-0.

[18] Shi H, Wei J, He C. Where, When, and How: Context-Dependent Functions of RNA Methylation Writers, Readers, and Erasers. Molecular Cell. 2019; 74: 640–650. https://doi.org/10.1016/j.molcel.2019.04.025.

[19] Deacon S, Walker L, Radhi M, Smith S. The Regulation of m6A Modification in Glioblastoma: Functional Mechanisms and Therapeutic Approaches. Cancers. 2023; 15: 3307. https://doi.org/10.3390/cancers15133307.

[20] Visvanathan A, Patil V, Arora A, Hegde AS, Arivazhagan A, Santosh V, *et al*. Essential role of METTL3-mediated m^6A modification in glioma stem-like cells maintenance and radioresistance. Oncogene. 2018; 37: 522–533. https://doi.org/10.1038/onc.2017.351.

[21] Huff S, Tiwari SK, Gonzalez GM, Wang Y, Rana TM. m^6A-RNA Demethylase FTO Inhibitors Impair Self-Renewal in Glioblastoma Stem Cells. ACS Chemical Biology. 2021; 16: 324–333. https://doi.org/10.1021/acschembio.0c00841.

[22] Cui Q, Shi H, Ye P, Li L, Qu Q, Sun G, *et al*. m^6A RNA Methylation Regulates the Self-Renewal and Tumorigenesis of Glioblastoma Stem Cells. Cell Reports. 2017; 18: 2622–2634. https://doi.org/10.1016/j.celrep.2017.02.059.

[23] Zhang S, Zhao BS, Zhou A, Lin K, Zheng S, Lu Z, *et al*. m^6A Demethylase ALKBH5 Maintains Tumorigenicity of Glioblastoma Stem-like Cells by Sustaining FOXM1 Expression and Cell Proliferation Program. Cancer Cell. 2017; 31: 591–606.e6. https://doi.org/10.1016/j.ccell.2017.02.013.

[24] Xu X, Zheng Y, Luo L, You Z, Chen H, Wang J, *et al*. Glioblastoma stem cells deliver ABCB4 transcribed by ATF3 via exosomes conferring glioblastoma resistance to temozolomide. Cell Death & Disease. 2024; 15: 318. https://doi.org/10.1038/s41419-024-06695-6.

[25] Zhang B, Wu Q, Li B, Wang D, Wang L, Zhou YL. m^6A regulator-mediated methylation modification patterns and tumor microenvironment infiltration characterization in gastric cancer. Molecular Cancer. 2020; 19: 53. https://doi.org/10.1186/s12943-020-01170-0.

[26] Li Y, Xiao J, Bai J, Tian Y, Qu Y, Chen X, *et al*. Molecular characterization and clinical relevance of m^6A regulators

across 33 cancer types. Molecular Cancer. 2019; 18: 137. https://doi.org/10.1186/s12943-019-1066-3.

[27] Cao Q, Chen Y. Integrated Analyses of m^6A Regulator-Mediated Methylation Modification Patterns and Tumor Microenvironment Infiltration Characterization in Pan-Cancer. International Journal of Molecular Sciences. 2022; 23: 11182. https://doi.org/10.3390/ijms231911182.

[28] Malta TM, Sokolov A, Gentles AJ, Burzykowski T, Poisson L, Weinstein JN, *et al*. Machine Learning Identifies Stemness Features Associated with Oncogenic Dedifferentiation. Cell. 2018; 173: 338–354.e15. https://doi.org/10.1016/j.cell.2018.03.034.

[29] Zheng XH, Zhou T, Li XZ, Zhang PF, Jia WH. Banking of Tumor Tissues: Effect of Preanalytical Variables in the Phase of Pre- and Postacquisition on RNA Integrity. Biopreservation and Biobanking. 2023; 21: 56–64. https://doi.org/10.1089/bio.2021.0124.

[30] Chen YY, Han QY, Chen QY, Zhou WJ, Zhang JG, Zhang X, *et al*. Impact of Sample Processing and Storage Conditions on RNA Quality of Fresh-Frozen Cancer Tissues. Biopreservation and Biobanking. 2023; 21: 510–517. https://doi.org/10.1089/bio.2022.0069.

[31] Zhang Y, Geng X, Li Q, Xu J, Tan Y, Xiao M, *et al*. m6A modification in RNA: biogenesis, functions and roles in gliomas. Journal of Experimental & Clinical Cancer Research: CR. 2020; 39: 192. https://doi.org/10.1186/s13046-020-01706-8.

[32] Tong F, Zhao JX, Fang ZY, Cui XT, Su DY, Liu X, *et al*. MUC1 promotes glioblastoma progression and TMZ resistance by stabilizing EGFRvIII. Pharmacological Research. 2023; 187: 106606. https://doi.org/10.1016/j.phrs.2022.106606.

[33] Yang J, Yan J, Liu B. Targeting EGFRvIII for glioblastoma multiforme. Cancer Letters. 2017; 403: 224–230. https://doi.org/10.1016/j.canlet.2017.06.024.

[34] Chistiakov DA, Chekhonin IV, Chekhonin VP. The EGFR variant III mutant as a target for immunotherapy of glioblastoma multiforme. European Journal of Pharmacology. 2017; 810: 70–82. https://doi.org/10.1016/j.ejphar.2017.05.064.

[35] Roth P, Weller M. Challenges to targeting epidermal growth factor receptor in glioblastoma: escape mechanisms and combinatorial treatment strategies. Neuro-oncology. 2014; 16: viii14–viii19. https://doi.org/10.1093/neuonc/nou222.

[36] Ezzati S, Salib S, Balasubramaniam M, Aboud O. Epidermal Growth Factor Receptor Inhibitors in Glioblastoma: Current Status and Future Possibilities. International Journal of Molecular Sciences. 2024; 25: 2316. https://doi.org/10.3390/ijms25042316.

[37] Li C, Pu B, Gu L, Zhang M, Shen H, Yuan Y, *et al*. Identification of key modules and hub genes in glioblastoma multiforme based on co-expression network analysis. FEBS Open Bio. 2021; 11: 833–850. https://doi.org/10.1002/2211-5463.13078.

[38] Ling YZ, Luo JR, Cheng SJ, Meng XP, Li JY, Luo SY, *et al*. GARNL3 identified as a crucial target for overcoming temozolomide resistance in EGFRvIII-positive glioblastoma. American Journal of Translational Research. 2024; 16: 1550–1567. https://doi.org/10.62347/TFUT3720.

[39] He H, Huang J, Wu S, Jiang S, Liang L, Liu Y, *et al*. The roles of GTPase-activating proteins in regulated cell death and tumor immunity. Journal of Hematology & Oncology. 2021; 14: 171. https://doi.org/10.1186/s13045-021-01184-1.

[40] Xiao H, Wang G, Zhao M, Shuai W, Ouyang L, Sun Q. Ras superfamily GTPase activating proteins in cancer: Potential therapeutic targets? European Journal of Medicinal Chemistry. 2023; 248: 115104. https://doi.org/10.1016/j.ejmech.2023.115104.

[41] Cao Y, Qiu G, Dong Y, Zhao W, Wang Y. Exploring the role of m^6 A writer RBM15 in cancer: a systematic review. Frontiers in Oncology. 2024; 14: 1375942. https://doi.org/10.3389/fonc.2024.1375942.

[42] Li C, Jiang X, Yuan Y, Wang Q. RBM15-mediated m^6A modification in cancer progression and tumor immunity: molecular mechanisms and therapeutic potential. Frontiers in Cell and Developmental Biology. 2025; 13: 1713615. https://doi.org/10.3389/fcell.2025.1713615.

[43] Wang X, Tian L, Li Y, Wang J, Yan B, Yang L, *et al*. RBM15 facilitates laryngeal squamous cell carcinoma progression by regulating TMBIM6 stability through IGF2BP3 dependent. Journal of Experimental & Clinical Cancer Research: CR. 2021; 40: 80. https://doi.org/10.1186/s13046-021-01871-4.

[44] Zhang Z, Mei Y, Hou M. Knockdown RBM15 Inhibits Colorectal Cancer Cell Proliferation and Metastasis Via N6-Methyladenosine (m6A) Modification of MyD88 mRNA. Cancer Biotherapy & Radiopharmaceuticals. 2022; 37: 976–986. https://doi.org/10.1089/cbr.2021.0226.

[45] Yuan J, Guan W, Li X, Wang F, Liu H, Xu G. RBM15 mediating MDR1 mRNA m^6A methylation regulated by the TGF β signaling pathway in paclitaxel resistant ovarian cancer. International Journal of Oncology. 2023; 63: 112. https://doi.org/10.3892/ijo.2023.5560.

[46] Jiang X, Liu B, Nie Z, Duan L, Xiong Q, Jin Z, *et al*. The role of m6A modification in the biological functions and diseases. Signal Transduction and Targeted Therapy. 2021; 6: 74. https://doi.org/10.1038/s41392-020-00450-x.

[47] Guo X, Qiu W, Wang C, Qi Y, Li B, Wang S, *et al*. Neuronal Activity Promotes Glioma Progression by Inducing Proneural-to-Mesenchymal Transition in Glioma Stem Cells. Cancer Research. 2024; 84: 372–387. https://doi.org/10.1158/0008-5472.CAN-23-0609.

[48] Li F, Chen S, Yu J, Gao Z, Sun Z, Yi Y, *et al*. Interplay of m^6 A and histone modifications contributes to temozolomide resistance in glioblastoma. Clinical and Translational Medicine. 2021; 11: e553. https://doi.org/10.1002/ctm2.553.